Physics 100/301, Lab 1

Hans Henken, Kevin Laube, Tony Li, Franklin Liou, Jake Zeller

Abstract

The purpose of *Lab 1: Introduction to the Equipment* was to introduce students to the student observatory, the 24″ student telescope and it associated instruments, the program software used to analyze data such as *TheSky* and *MaximDL*, and allow students to become confident in their abilities to gather, process and discuss data. The lab was broken up into three main sections to help familiarize students with the observational process. In the first section, we analyzed the limitations and characteristics of the CCD. This process involved taking two bias frames and using *Maxim* to determine read noise, and measuring average dark current in a dark frame. Then we observed two known stars, GSC4108:822, magnitude 9.86, and GSC4108:852, magnitude 14.1, to calculate the CCDs plate scale, field of view and angular resolution. The second section involved taking several images of an A star, SAO 13913, magnitude 9.21, to experiment with tricolor filters and the effects of sky brightness. Finally, we took tricolor images of M1, the Crab Nebula, and clear images of M51, the Whirlpool Galaxy, to experiment with taking images of extend objects.

1 Targets, Equipment and Methods

1.1 General Summary of Observational Technique

The telescope was cooled to -40 °C each night for optimal observation. Target stars and extended objects were located by inputting J2000 coordinates in to *TheSky*, which was directly connected to the telescope and focused it on the exact position in the sky. We then took a few low quality images to ensure the location was correct, after which we focused the telescope by minimizing the full width half maximum (FWHM) value for a star in our field. Finally, we took extended exposures, being careful to avoid saturating images with too much light. To improve image quality, it was important to account for bias and dark current. The bias was removed from frames by taking one 0s exposure and subtracting it from the final image. Dark frame exposure times varied to match the exposure time of the target object. The dark frame was later subtracted from the overall image. As a side note on the processing side, the dark frames included the bias from, so subtracting the dark frame accounted for the bias as well.

1.2 Innovative Set-ups, Observational Problems, and Experimental Challenges

Observations were taken over a span of 3 weeks. We experienced a variety of challenges, both from sky viewing and equipment setup standpoints. On the first night fog and cloud cover cut off observing time early and limited the focus of the telescope to a FWHM in the range of 5 to 6 pixels. Day 2 was clear, with little cloud cover, and humid. The humidity caused condensation to occur on the telescope which greatly affected the imaging quality of objects. Image quality improved when the telescope was heated to -30 °C instead of

Target	**Time**	**Exposure Time**	**Filter**	**Seeing Conditions**
GSC4105:822/852	2013-04-03 22:15 PDT	60	Clear	3.9″
GSC4105:822/852	2013-04-10 22:33 PDT	20	Slit Viewer	
SAO13913		5 15 15 15	Clear B G R	4.2″ (cloudy)
M1	2013-04-17 20:45 PDT	15 60 60 60	Clear B G R	2.4″ (half moon)
M51		30	Clear	3.0″

Table 1: Table of Observations.

its normal temperature of −40 °C. However, the FWHM was still limited to 6 to 7 pixels at best. More time was spent analyzing previous data then imaging new objects because of the limitations of the telescope. Day 3 was clear and the telescope was working properly. Final images were taken of our galactic and extragalactic objects and sky brightness was calculated. The telescope was cooled to its normal temperature of −40 °C and the FWHM was between 3.5 to 5 pixels. No set-up changes were made to the telescope.

2 Results and Analysis

2.1 Angular Resolution and Field of View

The angular resolution of a star is calculated by multiplying its full width at half maximum by the plate scale of the CCD. The plate scale for a CCD is given by the relationship $P = \theta/d$, where θ, measured in degrees, is the distance between two stars and d is the distance measured between the stars on the CCD in pixels. Our plate scale was calculated using the stars GSC4108:822 and GSC4108:852, which were known to have 4 arcminutes of separation. We obtained values of $d = 305$ and $\theta = 240$, which gave us a plate scale value of 0.787 arcsecond/pixel.

The theoretical plate scale value for a .61m telescope was calculated to be 0.811 arcsecond/pixel, which is slightly higher then the value we achieved. This is most likely due to the fact that measuring the exact distance between two stars is inaccurate was limited by the focus we were able to achieve. The poor focus led to the stars bleeding over into neighboring pixels, affecting our distance calculation. The plate scale was also used to calculate the field of view. Measured in pixels, the chip size was 1024×1024, which we multiplied by the square of the plate scale to obtain 649455.469 arcsecond^2. This process was repeated with the slit viewer camera and our calculated value for the plate scale was 0.47 arcsecond/pixel, with a field of view of 86184.135 arcsecond^2. Finally, the angular resolution of our two stars, GSC4108:822 and GSC4108:852, were calculated to be 4.171 arcseconds and 3.879 arcseconds. However, the theoretical value obtained for these two stars were 4.2983 arcseconds and 3.997 arcseconds. respectively. We found that our actual values were smaller than the theoretical values because of a similar problem that was faced with determining the plate scale. In theory, the FWHM value should be equal to 1 pixel per star. Since the CCD is unable to accurately measure a pixel per star, light from stars tend to bleed over into adjacent pixels which reduces the accuracy of the angular resolution.

2.2 Dark Current and Sky Brightness

Dark Current at 60s exposure (at $-39.6°$ C) $\rightarrow 28.38 \pm 226.182$ counts / pix $= .473 \pm 3.76$ cnts/p/s

Dark current at 60s exposure (at $-5°$ C) $\rightarrow 134.529 \pm 725.623$ counts / pix $= 2.23 \pm 12.08$ cnts/p/s

Sky Brightness (cnts/s/p)

- Clear: 20s = 16.85 5s = 16.7
- Red: 15s = 4.03, 60s = 7.89
- Green: 15s = 5.22, 60s = 11.36
- Blue: 15s = 2.51 60s = 2.11

Dark current and sky brightness are critical values to determine and subtract from our final image. To see how dark current changes with temperature we took two 60 second exposures at different temperatures. The first exposure was taken at a temperature of $-39.6°$ C and the second exposure was taken at a temperature of $-5°$ C. The values obtained for the dark current were 0.473 ± 3.76 counts/second/pixel and 2.242 ± 12.08 counts/second/pixel, respectively. From these observations, we can see that dark current is proportional to temperature. Theoretically, dark current should be proportional to $e^{-\Delta E/kT}$ where ΔE is the band gap of doped silicon, k is Boltzmanns constant, and T is the temperature of the CCD, where an increase in the temperature will increase the dark current, which matches our observations. When making observations, we not only collect light from astronomical objects, but also from stray photons from scattering of other light sources. This is known as sky brightness. In general we found dark current to be significantly smaller then measured sky brightness for the clear images and tricolor filters when dark current was measured at the cooler temperature. However, dark current measured on the larger temperatures had a much higher variation, which reduced the accuracy we would have been able to attain when calculating sky brightness. Thus, cooling the CCD correctly is very important for minimizing the dark current and calculating an accurate sky brightness. This is especially true for filtered images, since the average sky brightness was about equal to the average dark current measured at the warmer temperature. Thus, the sky brightness could potentially be unnoticeable for these filters. Finally, we noted that the sky was brightest with the clear filter, followed by green and red, and was significantly dimmer in blue.

2.3 Efficiency of the CCD

2.3.1 Theoretical Analysis

In order to characterize the efficiency of our CCD and each filter, we observed the photon flux of a type A0 star, SAO13913, and compared with the theoretical flux. The theoretical flux was calculated as follows:

First, we calculated the theoretical photon flux of each frequency band of SAO13913 using the fact that an A0 star at 26.4 lightyears has magnitude 0, and that SAO13913 has a magnitude of 8.9. Using the magnitude equation:

$$8.9 - 0 = -2.5 \log \frac{F_{1,b}}{F_{0,b}}$$

where $F_{1,b}$ is the theoretical photon flux of SAO13913 in frequency band b and $F_{0,b}$ is the theoretical photon flux of a magnitude 0 A0 star in band b. Our results are listed in Table 3.1 below.

Band	Flux of mag0 star (Jy)	Flux of SAO13913(Jy)	Theoretical Photon Flux (photons/m^2/s)
B	4000	1.10	7.71×10^7
V	3600	0.99	9.27×10^7
R	3060	0.84	5.88×10^7

Table 2:

2.3.2 Results

Our observed photon fluxes in each band are listed in table 3.2 below. The observation condition was fairly clear, but there was also substantial sky brightness due to half moon.

Band	Observed Photon Flux (photons/s)	Theoretical Photon Flux (photons/s)	Efficiency
B	4.10×10^4	2.24×10^7	0.183%
V	1.94×10^4	2.69×10^7	0.072%
R	1.98×10^4	1.71×10^7	0.116%

Table 3:

2.3.3 Error Analysis

We calculated our errors for the number of photons detected for each filter using the following formula:

$$\Delta I = [(3D \times t \times G) + (2 \times SB \times t \times G) + (A \times t \times G) + (4 \times \Delta I_r)]^{\frac{1}{2}}$$

where D is our average dark current of 0.43 counts/pixel/s; SB is the sky brightness; A is the astronomical signal; ΔI_r is our read noise of 0.95 counts/pixel; the observation time t is 60 seconds; our gain is 5.2 e/ADU. Our results are summarized in table 3.3.

Band	Observed Photon Flux (photons/s)	Efficiency
B	41000 ± 26.6	0.183%±0.001%
V	19400 ± 21.0	0.072%±0.001%
R	19800 ± 20.3	0.116%±0.001%

Table 4:

Our largest source of error was sky brightness. The possible sources for lost efficiency are absorption by the atmosphere, interstellar medium, and also the quantum efficiency of the CCD. The efficiency is higher in the B and R band.

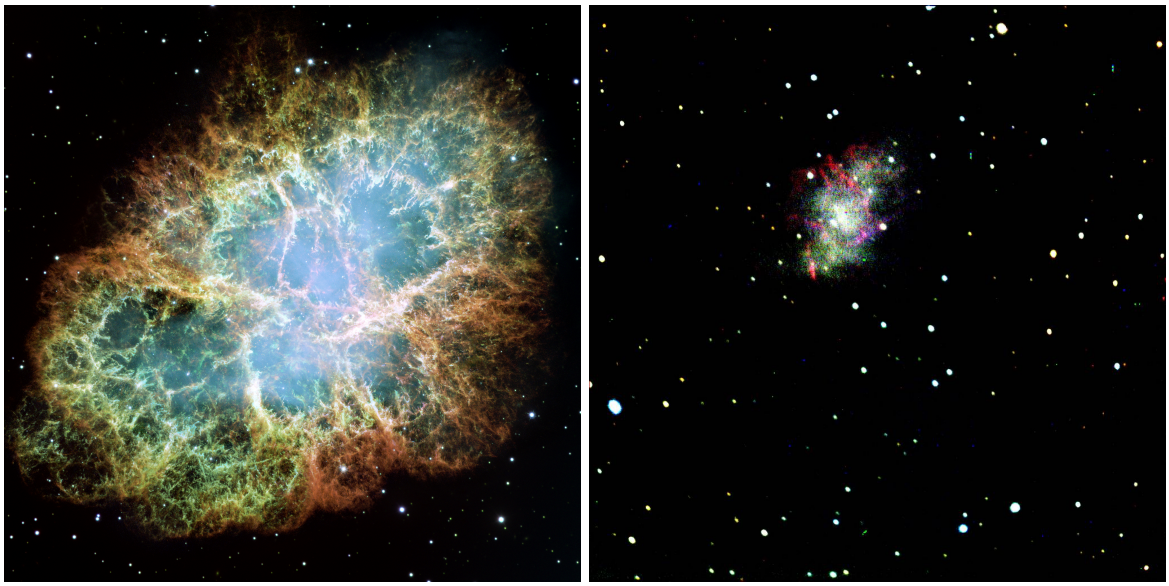

Figure 1: **Left**: Hubble image of the Crab Nebula. **Right**: Our composite image of the Crab Nebula.

2.4 Images of Galactic and Extra-Galactic Objects

2.4.1 M1: Crab Nebula

The Crab Nebula is a remnant of a supernova first observed in 1054 A.D. It spans about 10 light years across and contains a pulsar at its center. Notable features of the nebula from the Hubble image in Figure 1 include:

- Shape: The nebula has an extended, roughly oval shape with irregular edges.
- Color: From the Hubble image, we note that the interior of the nebula is characterized strongly by greens and blues, and in particular, the center appears to have a diffuse blue glow. In contrast, the edges of the nebula are characterized by redder, dusty edges.
- Filaments: We note dusty "fingers" in the image, extending from the edge inward to the center of the nebula. The filaments appear longer and sparser toward the center, and shorter and more dense towards the edges.

The shape of the object in our image, shown in Figure 1, is generally consistent with the Hubble image. In the Hubble image, one can clearly observe a diffuse blue–and to a lesser extent, green–center, and red edges. While our image contains the same colors and the red appears toward the exterior, we were unable to clearly observe the diffuse blue center. In addition, clear filaments are not visible in our image, as our telescope is unable to resolve structures on this scale. We note that we were only able to resolve stars to a FWHM of 3.2 pixels. With a plate scale of 0.787 arcsec/pix, this translates to a resolution of ~ 2.5 arcsec. While this is not enough to prevent us from observing some of the larger filaments in the nebula, it blurs out most of the smaller details and substructures.

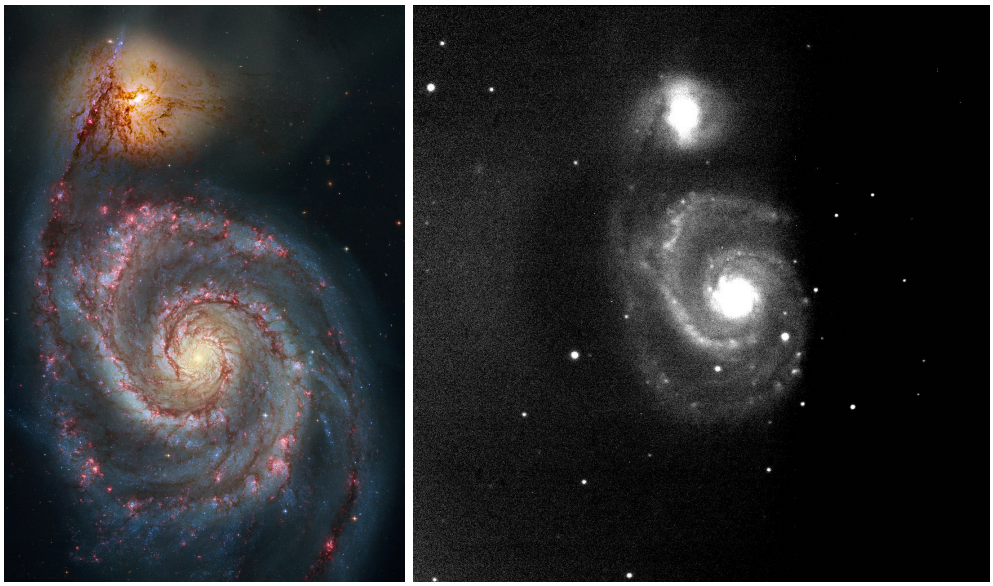

Figure 2: **Left**: Hubble image of M51. **Right**: Our image of M51.

2.4.2 M51: Whirlpool Galaxy

M51, the Whirlpool Galaxy, is located approximately 37 million light years from earth and was the first galaxy in which spiral structure was noted. The image in Figure 2 has multiple notable qualities:

- Shape: There appear to be two relatively distinct objects in the image. The larger of the two objects has a clear spiral structure and a bright center. The smaller of the two objects lies at the end of one of the spiral arms.
- Dust lanes: There are multiple thin, dark, dust lanes tracing the arms of the large spiral. The most notable dust lane seems to connect to the center of the smaller object.
- Runaway stars: There appears to be hazy material (runaway stars) being flung off the smaller object.

Figure 2 shows our image, in which we are able to distinctly resolve the two interacting objects in addition to the clear spiral structure of the larger object. Furthermore, we are able to observe the dark dust lanes, most notably the one extending into the smaller object. However, we are unable to unambiguously detect the runaway stars being flung off the smaller object, as it is below our noise threshold. There is substantial haze on the left side of the image, which we attribute to possible fog on the lens of the telescope or clouds which were entering the sky during the time of observation.

References

Bradt, Hale. Astronomy Methods : a Physical Approach to Astronomical Observations. Cambridge, UK: Cambridge University Press, 2004.

Ochsenbein F., Bauer P., Marcout J., 2000, A&AS 143, 221